



Still after decades of studying dwarf galaxies, the formation and evolution of these objects is considered an active debate. Here with high resolution multiplexing deep-SAMI data cubes and statistically significant sample of dEs in the Fornax cluster, we are studying kinematics, chemical composition and structure of these faint objects.

By comparing our spectroscopic results of 36 SAMI Fornax dwarf early-type galaxies and 15 giant ellipticals with literature (Toloba et al. 2014, & Facon-Barroso et al. 2011), we see that dwarfs and giants follow the same slope on Faber-Jackson relations and Fundamental Plane. This tight FJ relation suggests a same internal structure for Es and dEs, and the tight FP indicates that all of them are in Virial equilibrium. Moreover, the observed local DM fraction of cluster galaxies is the same as in the local group. With our deep, high-resolution spectroscopy we are able to probe to lower galaxy masses $M \sim 10^{7.4} M_{\odot}$ than previous studies.

I. Abstract

4. Sample & Data

5. Preliminary Science Results

The SAMI Fornax project started in 2015 with the Sydney-AAO Multi-Object Integral-field (SAMI) spectrograph on the Anglo-Australian Telescope (AAT), with the aim of studying the origin and the inner processes of dwarf galaxies inside Fornax cluster. We performed deep observations of 5-7 hours exposure time, observing 12 galaxies at the same time, during 3 observing runs in 2015B, 2016B and 2018B, resulting in 37 dwarf galaxies, 14 giant elliptical galaxies with good spectra.

SAMI is an integral-field spectrograph equipped by 13 fiber-based IFUs called hexabundles, and 26 pluggable sky fibers (Bryant et al. 2014). Each hexabundle with a field-of-view of 15'' diameter, is made of 61 1.6'' optical fibers. These hexabundles have physical size <1 mm, with a filling fraction of 73% and together with sky fibers each fits into pre-drilled holes in a field plate. The plug plate with about one degree field-of-view is installed at the AAT's Prime Focus Camera top end placing the face of hexabundle at the focal plane of the telescope.

To study the structure of low-mass galaxies such as dEs in the Fornax cluster, high resolution spectra and high S/N are needed. With 1500V gratings in blue and 100R gratings in red, our data has a resolution of ~ 5100 (FWHM = 1.0Å) in the blue ($\sim 4660 - 5430$ Å) and ~ 4300 (FWHM = 1.6Å) in the red ($6250 - 7350$ Å). This means potentially reaching around 25 km/s and 30 km/s velocity dispersion in blue and red respectively.

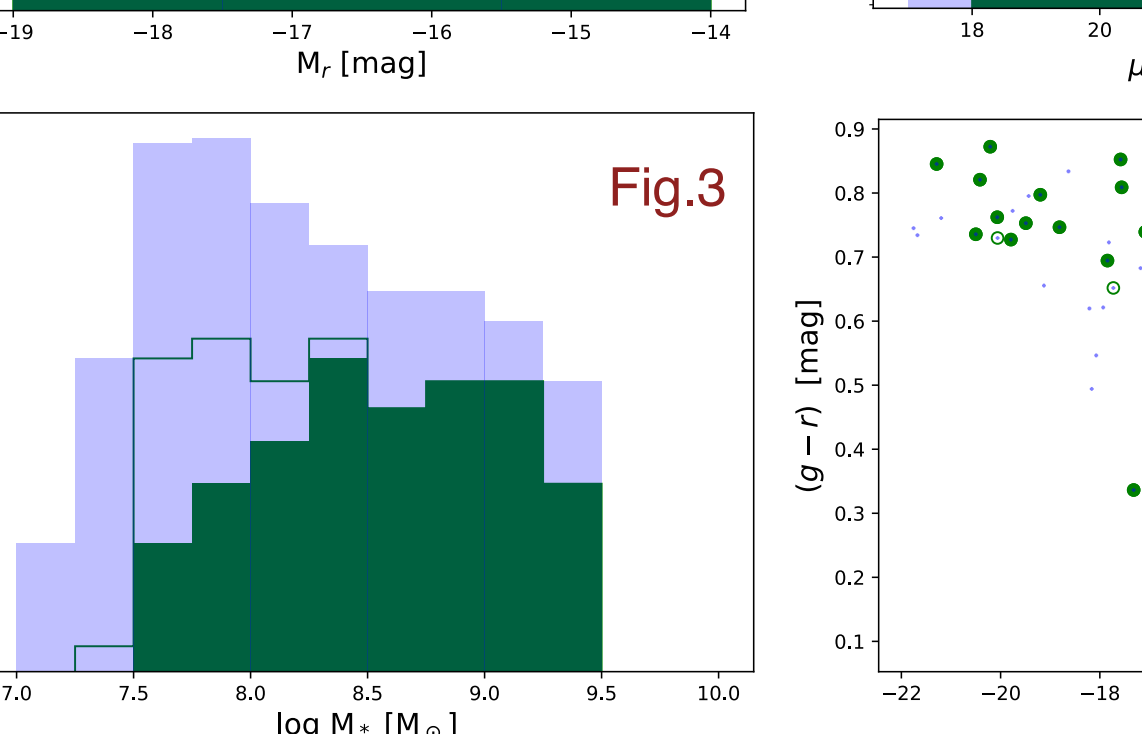
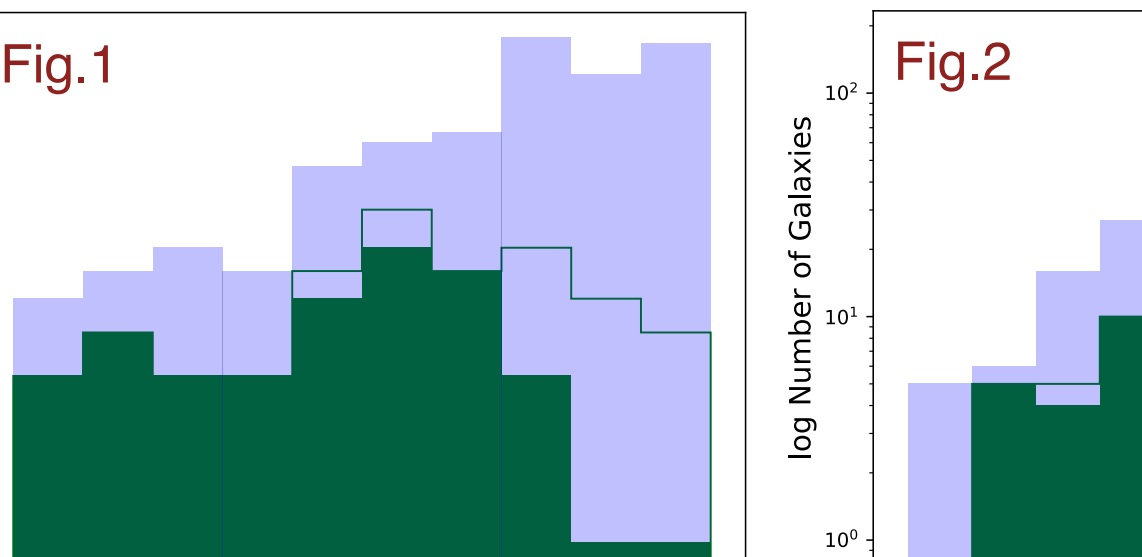


(Fig. 4) The color-magnitude diagram for our sample (green circles), compared to that from the full FDS sample (blue crosses). We primarily target galaxies on the red sequence, but do include some blue galaxies that satisfy our selection criteria.

2. Scientific Qs.

- Are dEs and giants galaxies follow the same scaling relations?(FP, FJ, etc.)
- What is the DM contents of faint cluster dEs?
- What is the physical role of the environment in the evolution of dEs?
- What is the fraction of rotational over pressure supported dEs?
- FUTURE WORK
- Can we detect the effects of starvation or ram-pressure on dEs?
- How do the stellar populations of dEs depend on the environment ?

3. Analysis

We extracted stellar kinematics and stellar population from absorption-line spectra of our galaxies by using the penalised Pixel Fitting (pPXF) routine of Cappellari & Emsellem (2004). pPXF basically is a maximum penalized likelihood approach in pixel space, with the aim of finding an optimal template with the minimum template-galaxy mismatch errors. It finds the best-fitting linear combination of input stellar templates by convolving them with the line-of-sight velocity distribution of the input galaxy's spectra, and then the best-fitting parameters are determined by a non-linear chi-squared minimization in pixel space (logarithmically binned in wavelength).

Moreover, we computed the uncertainties by (100 realizations) Monte Carlo simulations. In each loop the best-fitted spectrum is disturbed by random spectra convolved by the sigma of the difference between original and best-fitted template spectra. The best match for the SAMI-Fornax's wavelength range and spectral resolution is single-age single-metallicity population models of PEGASE-HR (Le Borgne et al. 2004). ELODIE is a high resolution stellar library of 1959 spectra for 1503 stars with R=10 000 at lambda=550 nm

4. Sample & Data

5. Preliminary Science Results

1. Angular-Momentum

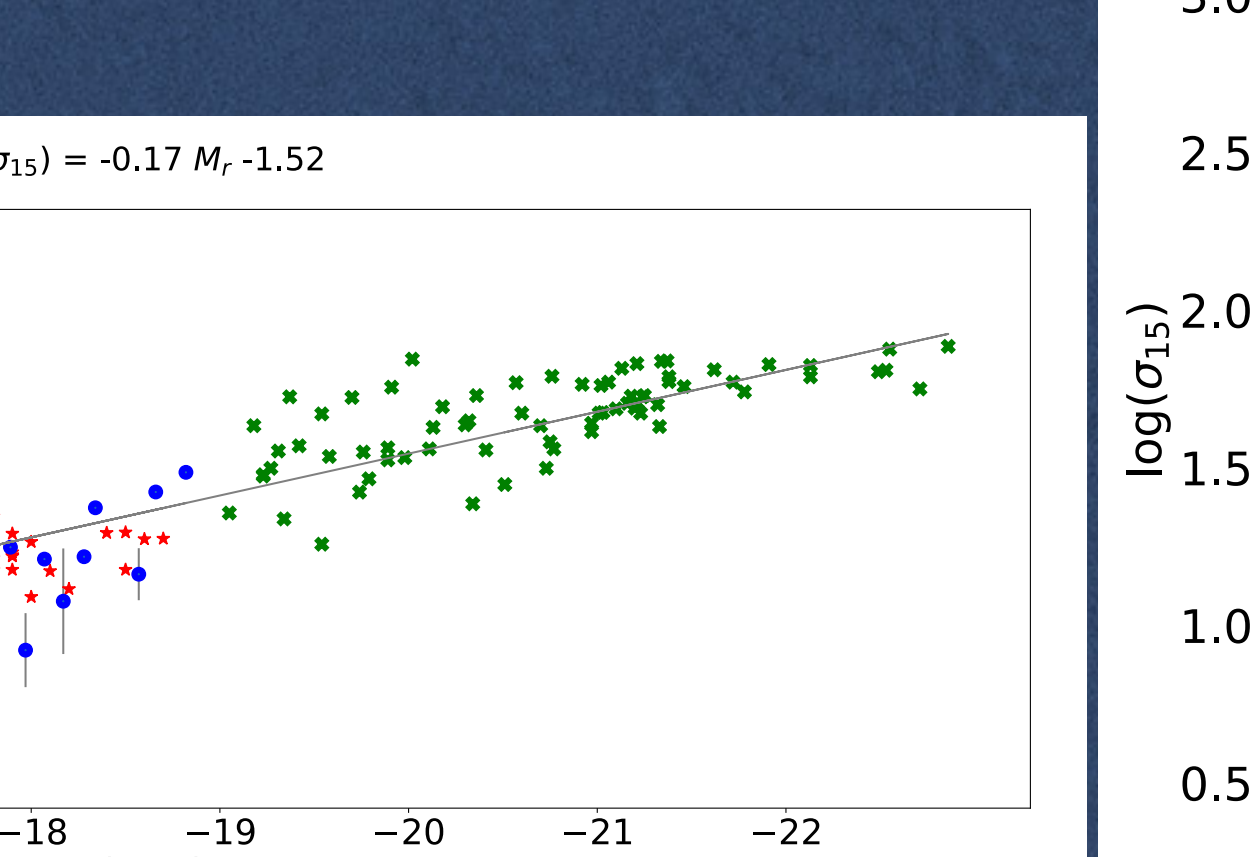
From our maps of stellar velocity and stellar velocity dispersion we measure λ_R , the specific stellar angular momentum, a proxy for the degree of rotational or pressure support within a galaxy. In the left figure we show profiles of λ_R vs r/R_e for galaxies of different stellar mass. For massive galaxies our radial coverage is limited, however for low mass galaxies we can trace the angular momentum out to relatively large radii. These profiles show a variety of behaviour – either rising rapidly then flattening at large radius or staying low at all radii. In the right hand figure we show the distribution of our galaxies in the λ_R - ellipticity plane. Galaxies below a $\lambda_R \sim 0.1$ are classified as slow rotators, systems with very low specific stellar angular momentum, often indicative of an evolutionary history involving significant dynamical interactions such as merging or harassment.



2. Faber-Jackson Relation

One of the first discoveries in early-type galaxies was that their stellar velocity dispersion correlates with their luminosity (Faber & Jackson 1967). This two dimensional relation $L \sim \sigma^2$ Faber-Jackson relation is in fact a projection of Fundamental Plane.

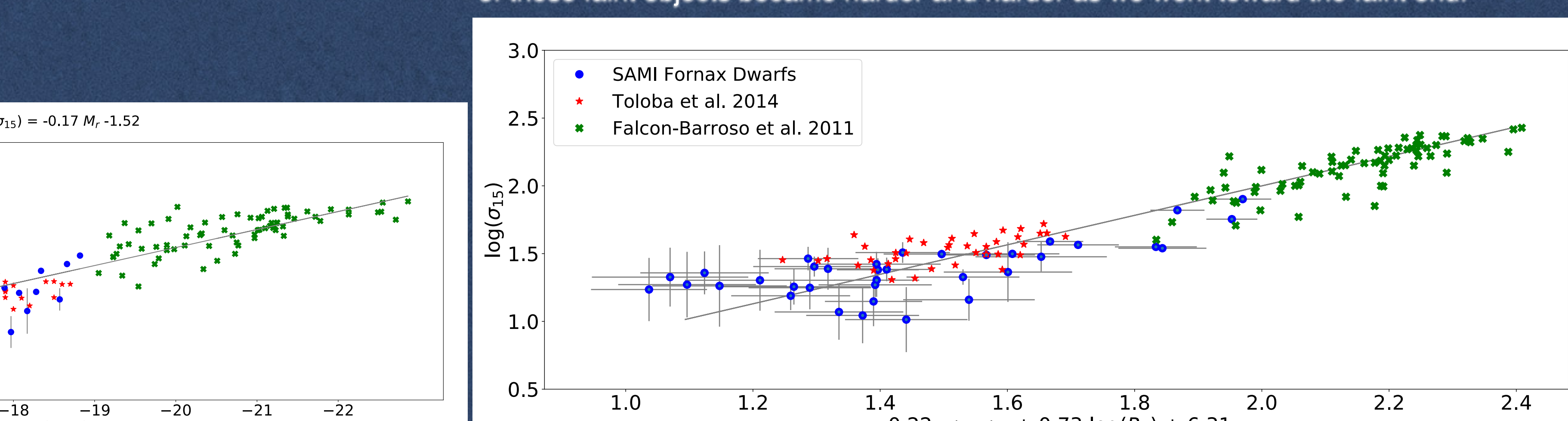
We see the same slope from giants to dwarf ellipticals, and so they seem to have same internal structure. As we go to fainter objects we continue to have tight relation.



3. Fundamental Plane

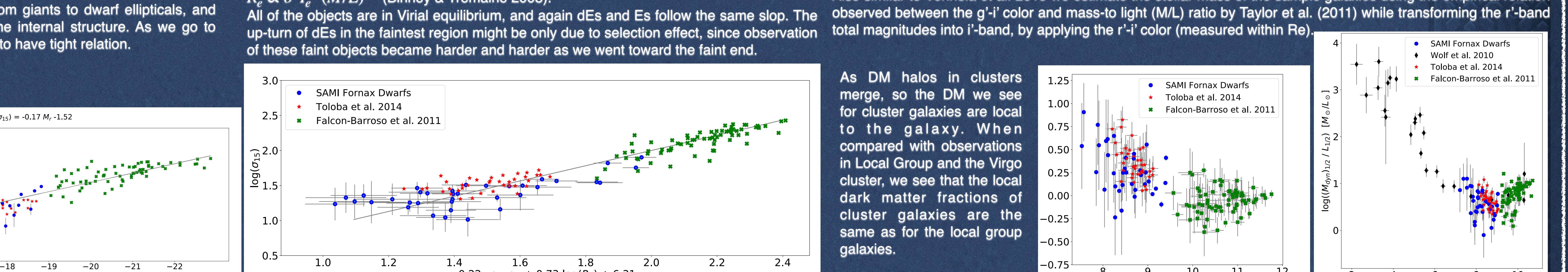
The empirical Fundamental plane which is a bivariate relation (Brosche 1973, Dressler et al. 1973 and Djorgovski & Davis 1987) between R_e (the half light ratio radius of the galaxy), I_e (the mean surface brightness within R_e in flux units), and σ (the galaxy internal velocity dispersion), is an indication of galaxies being in Virial equilibrium $R_e \propto \sigma^2 I_e^{-1} (M/L)^{-1}$ (Binney & Tremaine 2008).

All of the objects are in Virial equilibrium, and again dEs and Es follow the same slope. The up-turn of dEs in the faintest region might be only due to selection effect, since observation of these faint objects became harder and harder as we went toward the faint end.



4. Dynamical Mass vs. Stellar Mass

Not considering the difference between radial and tangential velocity dispersion weakens our ability to reach accurate conclusions about structure and formations of galaxies. This becomes more important in calculating dynamical mass of a galaxy by only having its 2d observed radial properties. Wolf et al. 2010 showed that within r_3 radius (where the log-slope of the 3D tracer density profile is -3) this difference is insignificant. Also similar to Venhola et al. 2019 we estimate the stellar mass of the sample galaxies using the empirical relation observed between the g'-i' color and mass-to light (M/L) ratio by Taylor et al. (2011) while transforming the r'-band total magnitudes into i'-band, by applying the r'-i' color (measured within R_e).



5. Kinematic Maps

The velocity and velocity dispersion maps of 5 representative SAMI-Fornax galaxies. The photometric pictures are taken from FDS catalog. The red circle is the field-of-view of SAMI which is 15'' diameter.

References

- Bryant J. J., et al. 2017, MNRAS, 474, 2857
Broche, P. 1989, A&A, 21, 359
Cappellari M., Emsellem E., 2004, Publ. Astron. Soc. Pacific, 116, 468
Djorgovski S., Davis M., 1987, ApJ, 313, 59
Dressler A., et al. 1987, ApJS, 63, 42
Faber S. M., Jackson R. B., 1976, ApJ, 204, 1787
Ferguson H., 1989, ApJ, 338, 367
Ferrarese L., et al. 2012, ApJS, 200, 4
Facon-Barroso J., et al. 2018, MNRAS, 475, 1787
Iodice E., et al. 2016, ApJ, 820, 42
Iodice E., et al. 2019, A&A, 631, 1
Le Borgne J., et al. 2004, A&A, 425, 851
Serra P., et al. 2019, arXiv:1907.08367, A&A, in press
Taylor E. N., et al. 2011, MNRAS, 418, 1587
Toloba E., et al. 2014, ApJS, 215, 37
Venhola A., et al. 2017, A&A, 608, A142
Wolf J., et al. 2010, MNRAS, 406, 1220
Zabel N., et al. 2019, MNRAS, 483, 2251